Technical University of Denmark

DTU

High-pulse energy supercontinuum laser for high-resolution spectroscopic photoacoustic imaging of lipids in the 1650-1850 nm region

Dasa, Manoj Kumar; Markos, Christos; Maria, Michael; Petersen, Christian Rosenberg; Moselund, Peter M.; Bang, Ole

Link back to DTU Orbit

DTU Library
Technical Information Center of Denmark

High-pulse energy supercontinuum laser for high-resolution spectroscopic photoacoustic imaging of lipids in the 1650-1850 nm region

Manoj Kumar Dasa,[1,*] Christos Markos,[1] Michael Maria,[1] Christian R. Petersen,[1] Peter M. Moselund,[2] and Ole Bang[1,2]

[1]*Department of Photonics Engineering, Technical University of Denmark, 2800 Kgs. Lyngby, Denmark*
[2]*NKT Photonics A/S, Blokken 84, Birkerød 3460, Denmark*
*manda@fotonik.dtu.dk

Abstract: We propose a cost-effective high-pulse energy supercontinuum (SC) source based on a telecom range diode laser-based amplifier and a few meters of standard single-mode optical fiber, with a pulse energy density as high as ~25 nJ/nm in the 1650-1850 nm regime (factor >3 times higher than any SC source ever used in this wavelength range). We demonstrate how such an SC source combined with a tunable filter allows high-resolution spectroscopic photoacoustic imaging and the spectroscopy of lipids in the first overtone transition band of C-H bonds (1650-1850 nm). We show the successful discrimination of two different lipids (cholesterol and lipid in adipose tissue) and the photoacoustic cross-sectional scan of lipid-rich adipose tissue at three different locations. The proposed high-pulse energy SC laser paves a new direction towards compact, broadband and cost-effective source for spectroscopic photoacoustic imaging.

References and links

1. M. H. Xu and L. V. Wang, "Photoacoustic imaging in biomedicine," Rev. Sci. Instrum. **77**(4), 041101 (2006).
2. L. V. Wang, "Multiscale photoacoustic microscopy and computed tomography," Nat. Photonics **3**(9), 503–509 (2009).
3. Y. Junjie and L. V. Wang, "Photoacoustic microscopy," Laser Photonics Rev. **7**(5), 758–778 (2013).
4. J. Weber, P. C. Beard, and S. E. Bohndiek, "Contrast agents for molecular photoacoustic imaging," Nat. Methods **13**(8), 639–650 (2016).
5. P. C. Beard and T. N. Mills, "Characterization of post mortem arterial tissue using time-resolved photoacoustic spectroscopy at 436, 461 and 532 nm," Phys. Med. Biol. **42**(1), 177–198 (1997).
6. S. Sethuraman, J. H. Amirian, S. H. Litovsky, R. W. Smalling, and S. Y. Emelianov, "Spectroscopic intravascular photoacoustic imaging to differentiate atherosclerotic plaques," Opt. Express **16**(5), 3362–3367 (2008).
7. J. Hui, R. Li, E. H. Phillips, C. J. Goergen, M. Sturek, and J. X. Cheng, "Bond-selective photoacoustic imaging by converting molecular vibration into acoustic waves," Photoacoustics **4**(1), 11–21 (2016).
8. P. Wang, P. Wang, H. W. Wang, and J. X. Cheng, "Mapping lipid and collagen by multispectral photoacoustic imaging of chemical bond vibration," J. Biomed. Opt. **17**(9), 096010 (2012).
9. K. Jansen, A. F. W. van der Steen, M. Wu, H. M. M. van Beusekom, G. Springeling, X. Li, Q. Zhou, K. K. Shung, D. P. V. de Kleijn, and G. van Soest, "Spectroscopic intravascular photoacoustic imaging of lipids in atherosclerosis," J. Biomed. Opt. **19**(2), 026006 (2014).
10. K. Jansen, M. Wu, A. F. W. van der Steen, and G. van Soest, "Photoacoustic imaging of human coronary atherosclerosis in two spectral bands," Photoacoustics **2**(1), 12–20 (2014).
11. T. J. Allen, A. Hall, A. P. Dhillon, J. S. Owen, and P. C. Beard, "Spectroscopic photoacoustic imaging of lipid-rich plaques in the human aorta in the 740 to 1400 nm wavelength range," J. Biomed. Opt. **17**(6), 061209 (2012).
12. Z. Piao, T. Ma, J. Li, M. T. Wiedmann, S. Huang, M. Yu, K. Kirk Shung, Q. Zhou, C. S. Kim, and Z. Chen, "High speed intravascular photoacoustic imaging with fast optical parametric oscillator laser at 1.7 μm," Appl. Phys. Lett. **107**(8), 083701 (2015).
13. T. Buma, B. C. Wilkinson, and T. C. Sheehan, "Near-infrared spectroscopic photoacoustic microscopy using a multi-color fiber laser source," Biomed. Opt. Express **6**(8), 2819–2829 (2015).
14. M. Wu, K. Jansen, A. F. W. van der Steen, and G. van Soest, "Specific imaging of atherosclerotic plaque lipids with two-wavelength intravascular photoacoustics," Biomed. Opt. Express **6**(9), 3276–3286 (2015).

15. C. Lin, V. T. Nguyen, and W. G. French, "Wideband near-I.R. continuum (0.7-2.1 µm) generated in low-loss optical fibres," Electron. Lett. **14**(25), 822–823 (1978).
16. M. Bondu, C. Brooks, C. Jakobsen, K. Oakes, P. M. Moselund, L. Leick, O. Bang, and A. Podoleanu, "High energy supercontinuum sources using tapered photonic crystal fibers for multispectral photoacoustic microscopy," J. Biomed. Opt. **21**(6), 061005 (2016).
17. E. Aytac-Kipergil, A. Demirkiran, N. Uluc, S. Yavas, T. Kayikcioglu, S. Salman, S. G. Karamuk, F. O. Ilday, and M. B. Unlu, "Development of a Fiber Laser with Independently Adjustable Properties for Optical Resolution Photoacoustic Microscopy," Sci. Rep. **6**(1), 38674 (2016).
18. T. Buma, N. C. Conley, and S. W. Choi, "Multispectral photoacoustic microscopy of lipids using a pulsed supercontinuum laser," Biomed. Opt. Express **9**(1), 276–288 (2018).
19. Y. N. Billeh, M. Liu, and T. Buma, "Spectroscopic photoacoustic microscopy using a photonic crystal fiber supercontinuum source," Opt. Express **18**(18), 18519–18524 (2010).
20. J. M. Dudley, G. Genty, and S. Coen, "Supercontinuum generation in photonic crystal fiber," Rev. Mod. Phys. **78**(4), 1135–1184 (2006).
21. C. Markos, J. C. Travers, A. Abdolvand, B. J. Eggleton, and O. Bang, "Hybrid photonic-crystal fiber," Rev. Mod. Phys. **89**(4), 045003 (2017).
22. C. Larsen, S. T. Sørensen, D. Noordegraaf, K. P. Hansen, K. E. Mattsson, and O. Bang, "Zero-dispersion wavelength independent quasi-CW pumped supercontinuum generation," Opt. Commun. **290**, 170–174 (2013).
23. M. Maria, I. Bravo Gonzalo, T. Feuchter, M. Denninger, P. M. Moselund, L. Leick, O. Bang, and A. Podoleanu, "Q-switch-pumped supercontinuum for ultra-high resolution optical coherence tomography," Opt. Lett. **42**(22), 4744–4747 (2017).

1. Introduction

Photoacoustic imaging (PAI) is a hybrid imaging modality offering label-free high contrast imaging combined with high spatial resolution based on the wavelength-dependent molecular absorption and ultrasonic detection, respectively [1]. The ability of PAI to discriminate various endogenous agents using absorption contrast makes it a promising technique for the detection, diagnosis, and monitoring of various diseases [2–4]. Lipids are such key endogenous agents inside the body, as they act as major contrast agents in the identification of fatal chronic diseases like atherosclerosis and myocardial infarction [5].

The wavelengths used for PAI in most of the aforementioned cases fall in the ultra-violet to visible (UV-VIS) part of the electromagnetic spectrum due to the prominent absorption of the major endogenous agents like hemoglobin, melanin, etc [3]. Therefore, most of the early studies on lipids have also been focused on PA detection in the 420-530 nm [5] and 680-900 nm wavelength range [6]. Operation in the UV and VIS part of the spectrum provides a high spatial resolution but limited penetration depth, due to strong absorption of hemoglobin inside the blood, thereby, enabling the need for saline flush during the imaging. One possible way to achieve higher penetration depths is to operate at longer wavelengths. Especially in the second and first overtone transition bands of C-H bonds in lipids (1100-1300 and 1650-1850 nm) [7–11] where the absorption spectrum of lipid show well-differentiated peaks with higher absorption than other main constituents of biological tissue, such as water and hemoglobin [7,10], as illustrated in Fig. 1. Moreover, the lower absorption of hemoglobin eliminates the need for saline flush during the imaging of the lipids [11]. The absorption of lipid is the highest in the first overtone transition of C-H bond region (1650-1850 nm), making it the preferred band for PAI, in particular, intravascular PA (IVPA) imaging [10,14].

Photoacoustic Imaging of lipids in the first overtone region have been performed using optical parametric oscillators (OPO's) at a single wavelength (1725 nm) [12] and spectroscopic PA in the whole 1620-1780 nm band to identify different lipids [14]. However, while allowing a full band tunability, tunable OPO's have a high cost and a large footprint, making them not ideal for portable spectroscopic PAI systems. The other types of sources which could circumvent the use of OPO's up to some extent are based on stimulated Raman scattering (SRS). Such a source pumped at 1064 nm, below the zero-dispersion wavelength (ZDW) of the fiber, with isolated wavelengths or Raman orders at 1117, 1175, and 1238 nm has been used for lipid detection in the second overtone region [13]. However, as the pulse energy density (PED) decreases significantly with the order of the Raman line, the SRS-based

source has only a small number of isolated laser lines with enough pulse energy and does therefore not allow high-resolution spectroscopic PAI.
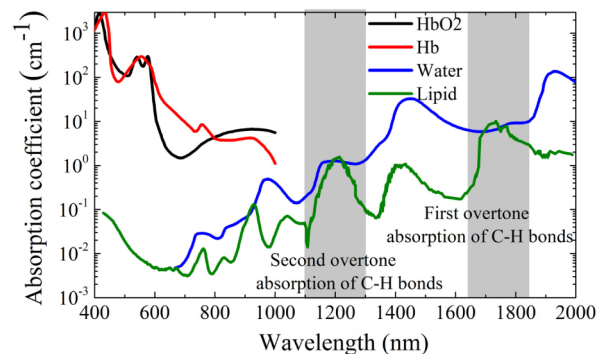

Fig. 1. Absorption coefficients of major endogenous agents (oxygenated hemoglobin (HbO2), deoxygenated hemoglobin (Hb), water, and lipid) inside the biological tissue. The inset shows the first and second overtone transition of C-H bond regions in the lipid molecules. (HbO2, Hb, and water are plotted based on the data from http://omlc.org/spectra/index.html and lipid from Ref [7].)

Interestingly, an SRS source can be made using a fiber with a ZDW close enough to the pump to allow one of the Raman lines to cross the ZDW and generate a supercontinuum (SC). Unfortunately, such an SC will then have low PED because the Raman lines take most of the energy [15,17]. Nevertheless, such a Raman SC source was recently used in a very nice study on multispectral PAI of lipids [18]. The source used a 1047 nm based Nd: YLF Q-switched laser to pump a photonic crystal fiber (PCF) with a ZDW at 1200 nm to generate Raman lines at 1098 and 1153 nm, and then an SC from 1200 to 1800 nm. Naturally, the SC had a low PED of only 320 nJ /50 nm (6.4 nJ/nm) at 1714 nm, making it necessary to use broad 50 nm filters to have enough energy to excite the PA signal. The low energy meant that PAI could not be done above 1714 nm, i.e. could not cover the most important wavelength of 1720 nm of maximum absorption of lipids [18]. In addition, a long length of 30 meters PCF (at $194/meter, price from Thorlabs) had to be used, which makes the source very expensive.

Importantly the state-of-the-art SC-based PAI studies [18] imply that spectroscopic PAI of lipids in the first overtone region (i.e. with more than 1 wavelength), has not yet been demonstrated. In addition only fixed broadband 50 nm filters have been used, where in order for spectroscopic PAI to take real advantage of the SC source; one has to be able to use it with a tunable narrow band filter to achieve high-resolution.

Here we propose a cost-effective high-pulse energy SC source for spectroscopic PAI, using a 1550 nm diode laser-based amplifier and a few meters of standard single mode optical fiber (SMF) (SMF28 at <0.2$/meter from Corning). We obtain an SC source with a maximum PED of 25 nJ/nm and enough pulse energy for PAI in the whole first overtone region, which at the moment is a record PED among reported SC sources used in a PAI study. The length of the fiber (3 meters) was tailored to have an almost flat PED (25 nJ/nm) profile in the central region 1725-1775 nm.

Using this SC source and a linear variable filter (LVF) of bandwidth 37-41 nm we here demonstrate spectroscopic PA studies of lipids in the first overtone region. We show that the system is able to image lipids and spectrally differentiate between two types of lipids (lipids in adipose and cholesterol). The high-pulse energy of the SC source would have allowed using 5 nm excitation bands and still have about 100 nJ on the sample as required for the typical optical resolution photoacoustic microscopy (OR-PAM) applications [19], but the LVF was the tunable filter with the narrowest bandwidth we could find commercially with a transmission efficiency >60% in this wavelength region. However, our SC source has enough PED to allow the use of more narrowband filters, for example, Acousto-Optic Tunable Filters

(AOTFs) and diffraction gratings, to potentially improve the spectral resolution of the spectroscopic PAI system.

2. Methods

2.1 High-pulse energy supercontinuum laser source

Figure 2(a) shows a schematic of the SC laser source. The laser system primarily consists of a fiber-coupled directly modulated laser diode based amplifier operating at 1550 nm (MLT-PL-R-OEM20, Manlight), with pulse duration 3 ns (FWHM) and energy of about 30 μJ at a repetition rate of 30 kHz, driven by an external function generator (TG2000, AIM-TTi).

The pulses from the laser are used to pump a standard commercially available SMF. The fiber has a numerical aperture of 0.14 and a ZDW close to 1300 nm, resulting in the anomalous dispersion at the pump wavelength, which is important for standard SC generation [20, 21]. In order to avoid back reflections from the end facet of the fiber, a bend filter was implemented and the fiber was angle cleaved (setting a cleaving angle of 8° in the tension cleaver (CT-100, Fujikura)), and then FC/APC connectorized for ease of handling.
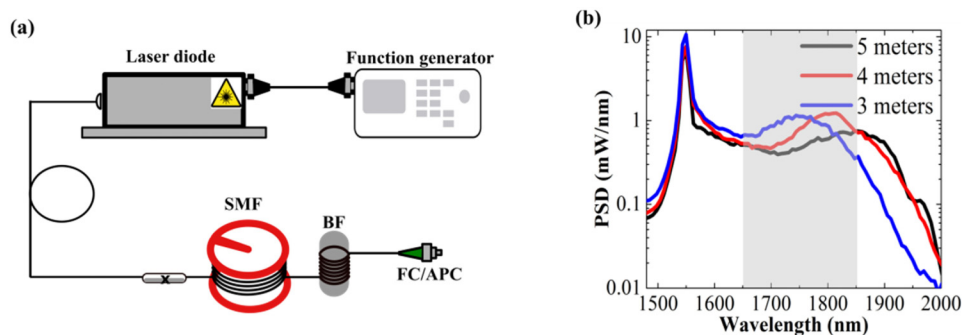

Fig. 2(a). Schematic of the high-pulse energy SC laser source. A function generator is used to drive directly modulated 1550 nm diode-laser based amplifier, with pulse duration 3 ns, and a repetition rate of 30 kHz. The output from the laser is used to pump a standard SMF. A bend filter (BF) is implemented and the fiber is angled cleaved and FC/APC connectorized, so as to eliminate back reflections from the end facet. Fig. 2(b). Power spectral density (PSD) of SC spectra generated by pumping an SMF of different length. The highlighted region is showing the first overtone transition of C-H bond region in lipids (1650-1850 nm).

The nanosecond (ns) pump pulse duration was chosen as a requirement for efficient PAI [16]. Commercial sources using ns pumping do exist, such as the SuperK Compact from NKT Photonics. These use a PCF as the nonlinear fiber and a pump close to the ZDW to generate a spectrum reaching below 500 nm to above 2300 nm. They typically have too little PED for PAI because the pump pulse energy is too weak and only a small part of the broad spectrum is within the region of interest to a given PAI experiment. We optimize the PED of our source by using high-pump pulse energy of 30 μJ and by using an SMF with a ZDW far below the pump. This means that a ns pulse will only generate spectral broadening above the pump wavelength [22], as is also seen in Fig. 2(b), and that the spectrum can be designed by an appropriate choice of the fiber length.

Three different lengths of SMF were tested (5, 4 and 3 meters) and the PSD of the SC output spectra were measured using an array spectrometer (NIRQuest512, Ocean Optics). The output spectra of the SC generated in all the three cases are shown in Fig. 2(b). In this work, we want to use spectroscopic PAI to study lipids in the first overtone region. From Fig. 2(b), it can be seen that 3 meters of fiber is then close to ideal for an optimum coverage of the 1650-1850 nm band by the SC spectrum.
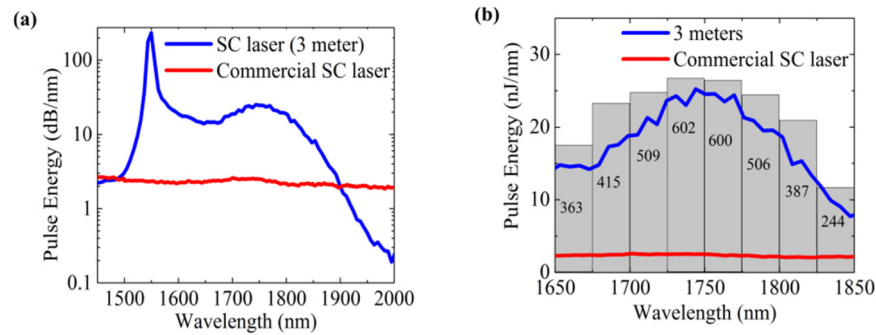
Fig. 3. Output spectrum of high-pulse energy SC laser source (a) PED of home built SC laser (3 meters of SMF) in comparison with commercial SC laser (b) PED of the SC laser in the first overtone region (3 meters of SMF) in comparison with the commercial SC laser, the inset shows the measured pulse energies (nJ) in 25 nm bands.

In Fig. 3(a) we show the corresponding PED of the SC source with 3 meters SMF, from which we can see that the PED of our source is an order of magnitude higher than the state-of-the-art ns-pumped commercial SC laser (SuperK Compact, NKT Photonics). Figure 3(b) shows the same comparison in the first overtone region of lipids. The vertical bars show the measured pulse energies (nJ) in 25 nm bands, which are sufficiently high for typical optical resolution based PAI [13,16,19].

2.2 Pulse-to-pulse stability of the high-energy SC laser source

The pulse-to-pulse stability of the laser source plays an important role in OR-PAM. We have characterized it by measuring the wavelength-dependent relative intensity noise (RIN), defined as RIN = $\sigma_M / \langle M \rangle$, where $\langle M \rangle$ is the mean peak power and σ_M is the standard deviation of the time series of peak powers. The light from the SC source is filtered using the LVF, detected using a 125 MHz InGaAs optical receiver (1811-FS, Newport) and a fast oscilloscope (HDO9404, Teledyne LeCroy).
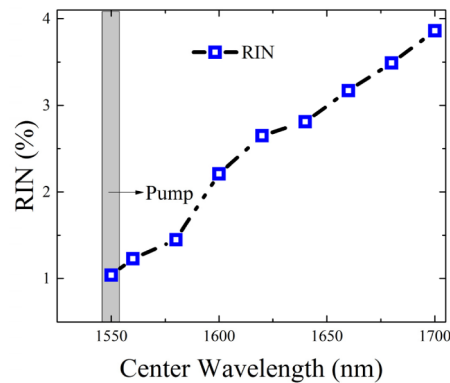

Fig. 4. Spectral profile of the Relative Intensity Noise (RIN) of the high-energy SC laser source, measured using the LVF.

The RIN was measured from 1550 nm to 1700 nm, as the upper limit of the photodiode's responsivity used for measurement was 1700 nm. 3000 pulses were recorded at each filter wavelength and used for the statistics. The spectral profile of the RIN is shown in Fig. 4, from which we see that the SC source has a low RIN of about 1.04-3.8%, which is lower than the noise of a similar, but lower pulse energy commercial source [23].

2.3 Spectroscopic photoacoustic imaging system

The experimental setup of the transmission-based spectroscopic PAI system is shown in Fig. 5. The system employs the aforementioned high-pulse energy SC laser source (with 3 meters of SMF) in conjunction with an LVF as the tunable excitation source. The output from the laser is collimated using an aspheric lens (L1) (A220TM, Thorlabs) and then sent to the LVF (Vortex Optical Coatings Ltd), which covers from 1200 nm to 2500 nm with a bandwidth of around 2% of the center wavelength. The filtered light is then steered using the mirrors (M1, M2, and M4) and focused on the sample using a 5x objective lens (L2). A flip mirror mount, a biconvex lens (L3), and a CCD camera are used to optically image and align the sample using ambient light. The major part of the excitation is built in a cage system, in order to make the setup compact and robust.

The generated PA signal is detected using a commercial 25 MHz ultrasonic focused transducer (Optel, Poland), with a 3 mm lead zirconate titanate (PZT) crystal as the piezoelectric active element. The acquired signals are filtered by a low pass filter (BLP-50 + , Mini-Circuits), amplified using two cascaded low-noise wideband signal amplifiers (ZFL-500LN, Mini-Circuits) and are then sent to an oscilloscope (HDO9404, Teledyne Lecroy). Phantoms are placed in a dish, with a 1 mm thick microscope slide fixed at the bottom of the dish, so that the dish is transparent to the optical excitation. The Phantoms are immersed in distilled water, which acts as a coupling medium for the generated acoustic waves. An x-y-z high precision stage is used for the alignment of the transducer with the confocal plane of the excitation and detection.
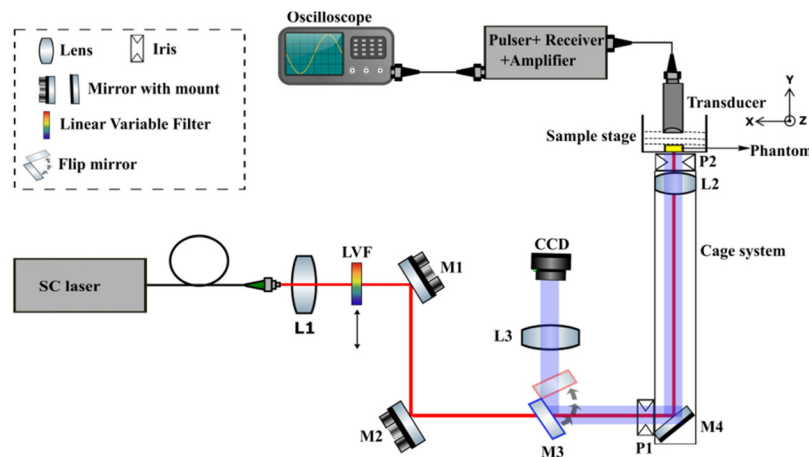

Fig. 5. Schematic of the spectroscopic PAI system. The fiber-coupled SC laser is used an excitation source, the light from the laser is collimated using an objective lens (L1). The excitation wavelength is filtered using an LVF. The filtered light is steered using the mirrors (M1, M2, and M4) and then focused on the phantom using an objective lens (L2). The generated PA signal is detected using a focused transducer, amplified using low-noise amplifiers and then sent to an oscilloscope. P1 and P2 are pinholes. A flip-mirror (M3), a lens (L3) and a CCD are used to align the sample.

The resolution of the spectroscopic PAI system was characterized by imaging the edge of an element (element 4 of group 3) in a 1951 USAF resolution target and is shown in Fig. 6. The edge spread function (ESF) was calculated by fitting the raw PA data collected from scanning the edge in steps of 2 µm. The line spread function (LSF) was then calculated by taking the derivative of the ESF. The lateral resolution of the system is defined as the full width at half-maximum (FWHM) of the LSF. The lateral resolution of the system was estimated to be about 11.8 µm.
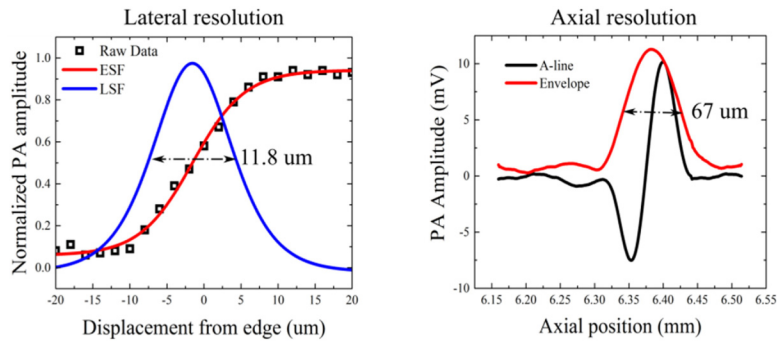
Fig. 6. Spatial resolution test of the spectroscopic PAI system. (a) Lateral resolution estimated by using the edge and line spread functions. (b) The axial resolution of the system estimated using the FWHM of the A-line envelope

The axial resolution of the system is calculated from the FWHM of the A-line envelope obtained from the USAF target and estimated to be about 67 μm.

3. Results

3.1 Differentiation of lipids using photoacoustic spectroscopy

Photoacoustic spectra of two different lipids (commercial grade cholesterol (C8667, Sigma-Aldrich) and the lipid in adipose tissue (collected from the abdominal tissue of chicken) were measured in 1600-1800 nm wavelength range, with a step size of 20 nm. The excitation bands filtered using LVF and their FWHM and the pulse energies with respect to the center wavelength are shown in Fig. 7(a) and Fig. 7(b) respectively. It can be observed from Fig. 7(b) that the measured pulse energies of the excitation bands (>380 nJ) are sufficiently high to excite PA signal.
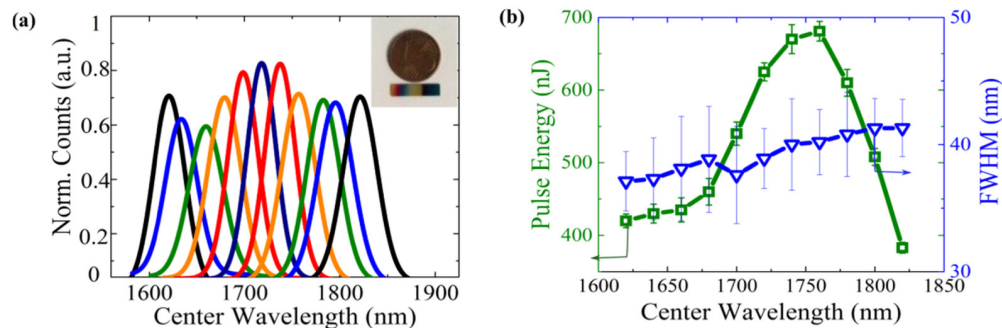

Fig. 7. Characterization of the LVF. (a) The filtered output of the SC source using the LVF in selected positions. The inset shows an optical photograph of the LVF. (b) Corresponding FWHM bandwidth and pulse energies. The error bars show the measured standard deviation of FWHM and pulse energies.

Photoacoustic signals detected by the transducer are low-noise amplified (58 dB), averaged over 1000 pulses, and normalized to (1) a reference measurement with only distilled water and no sample, and (2) to the respective maxima. The PA signal was averaged over 1000 pulses so as to further reduce pulse-to-pulse fluctuations and measure the PA spectra with higher SNR. The PA spectra of the two lipids are shown in Fig. 8, from which we see that there are distinct differences in the profile, with the maximum being at 1700 nm for Cholesterol and 1720 nm for Adipose tissue, due to the difference in their molecular structure and thus absorption spectra.
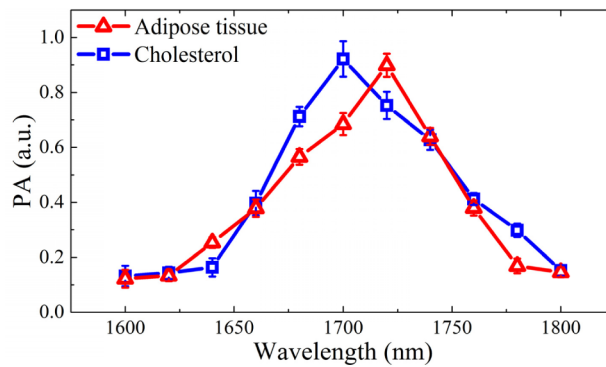
Fig. 8. Photoacoustic spectra (arbitrary units) of lipids in commercial grade cholesterol and adipose tissue, normalized to a reference spectrum with no sample, i.e., only with distilled water, and to the respective maxima.

3.2 Detection of lipid using photoacoustic imaging

Finally, we want to demonstrate the ability of our PAI system to do coarse cross-sectional scans of lipid-rich structures and extract accurate dimensions. The scan was done at a single wavelength by moving the sample in steps of 250 µm. The sample was a lipid-rich adipose tissue from the abdominal tissue of chicken and cut into 2.5mm slices using a razor blade. The 1720 nm band with maximum absorption (see Fig. 8) was chosen as excitation wavelength and the measured pulse energy at the sample plane was about 650 nJ.
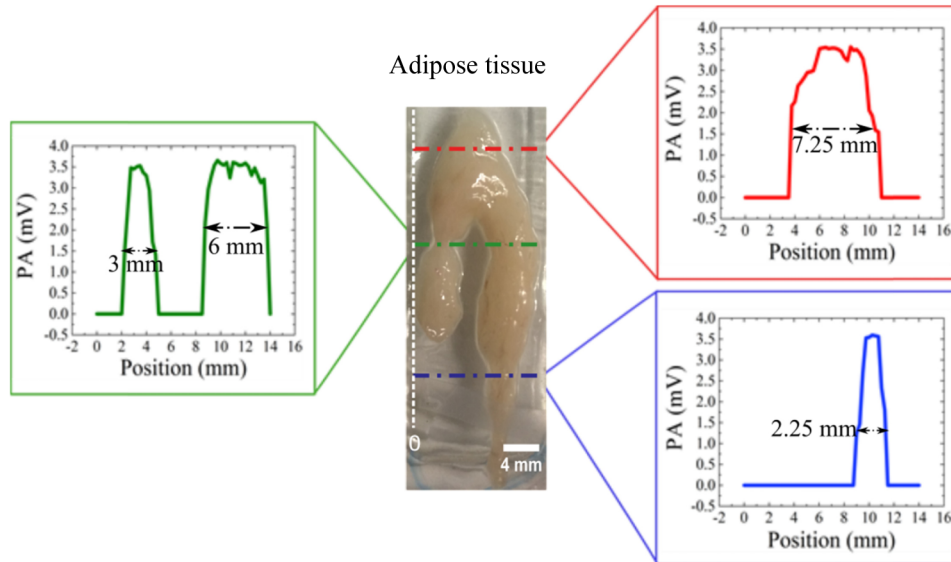

Fig. 9. Optical image of the lipid-rich adipose tissue from chicken. Insets show photoacoustic cross-sectional scan profiles along the dotted red, green, and blue lines on the image.

The detected PA signals at every excitation point of the sample were low-noise amplified, averaged over 100 pulses and normalized with the reference signal (obtained without the sample). The signal to noise ratio measured at this excitation wavelength is 20.89 dB. From Fig. 9 it can be clearly observed that the structural information of the tissue can be obtained from the PA cross-sectional scans. The dimensions obtained from the PA measurements across the red, green, and blue lines were 7.25 mm, 3 and 6 mm, and 2.25 mm respectively, all with an accuracy of 0.25 mm. The corresponding microscope (Axioskop, Carl Zeiss)

measurements of the dimensions were approximately 7 mm, 3 and 6 mm, and 2.50 mm, respectively. The slight disagreement is due to the difficulty in finding the exact same line between the microscope and PA scan. The PAI system is thus able to determine the physical dimensions.

4. Conclusion

In summary, we have demonstrated the development of a novel cost-effective high-pulse energy SC laser source for spectroscopic PAI in the first overtone transition band of C-H bond of lipids (1650-1850 nm). The SC source, which is based on 3 meters of standard telecom range SMF and a diode laser-based amplifier, is designed to have its maximum PED of 25 nJ/nm in the center of the region at 1725-1775 nm. This is factor >3 times higher than the so far record PED used for PAI in this spectral region [18]. The output PED of the SC can further be scaled by using additional amplifiers or pump sources with higher peak powers, with the scaling factor ultimately limited by the damage threshold of the fiber [16].

The high-pulse energy SC source, in conjunction with a tunable LVF of bandwidth 37-41 nm, allowed us to demonstrate spectroscopic PA measurements of lipid using an SC source for the first time in the first overtone transition band of C-H bonds (1650-1850 nm). In particular, we demonstrated spectroscopic differentiation of lipids in cholesterol and adipose tissue and the PA cross-sectional scans of lipid-rich adipose tissue at three different locations.

Disclosures

The authors declare that there are no conflicts of interest related to this article.